In Situ Analysis of Metal Melts in Metallurgic Vacuum Devices by Laser-Induced Breakdown Spectroscopy

J. GRUBER, J. HEITZ,* N. ARNOLD, D. BÄUERLE, N. RAMASEDER, W. MEYER, J. HOCHÖRTLER, and F. KOCH

Applied Physics, Johannes-Kepler University Linz, A-4040 Linz, Austria (J.G., J.Heitz, N.A., D.B.); VOEST-ALPINE Industrieanlagenbau, A-4031 Linz, Austria (N.R.); and BÖHLER Edelstahl, A-8605 Kapfenberg, Austria (W.M., J.Hochörtler, F.K.)

We report on rapid *in situ* analysis of liquid metal melts under reduced ambient pressure by laser-induced breakdown spectroscopy (LIBS) using a transportable system. LIBS denotes a method in which characteristic optical emission line intensities of excited species in laser-generated plasma plumes are used for a quantitative chemical analysis of target materials. It is a fast, noncontact method that can be carried out under various atmospheric conditions, allowing large working distances between the sample under investigation and the detection system. For these reasons, LIBS is applicable in particular for process control in metallurgy under reduced ambient pressure. This was demonstrated for two types of vacuum devices under production conditions at a steel mill. The results of these experiments, including calibration curves for Cr, Ni, and Mg in liquid steel, are presented. The influence of variations in the ambient pressure on the results of the LIBS analysis is discussed within the frame of a generalized shock-wave model for the expansion of the laser-induced plasma plume.

Index Headings: **LIBS; Laser-induced breakdown spectroscopy; Steel analysis; Laser-produced plasmas; Shock wave model; Ambient atmosphere and pressure; Chromium; Nickel; Manganese; Carbon; Titanium.**

INTRODUCTION

The standard procedure for process control in metallurgy involves several steps, including drawing a sample from the melt, transport to the laboratory, sample preparation, and finally the analysis of up to 30 elements. Many processes in secondary metallurgy are performed under a reduced pressure p of, typically, 0.01 to 5 mbar. The purpose is mainly the reduction of gaseous compounds (as, e.g., H_2) and sulfur (achieved by slag interaction) from the melt. Here, the drawing of samples is especially complicated because it requires either an interruption of the process (opening of the device, drawing of the sample, and renewed evacuation) or the use of an automatic sample drawing system in combination with a vacuum-sluice. A significant reduction of the time necessary to gain information about the composition of the melt can be achieved by analyzing the liquid metal directly in the ladle. For vacuum degassing processes, the direct monitoring of the carbon, sulfur, and eventually hydrogen content would be of the largest importance.

An *in situ* analysis of steel in metallurgic vacuum devices requires a fast, noncontact, and reliable method with no need for any sample preparation. Laser-induced breakdown spectroscopy (LIBS) meets these demands. A pulsed laser beam is focused onto the sample, resulting in plasma formation above the target surface. The spectroscopic investigation of the light emitted by the excited species in the plasma plume permits the quantitative determination of the sample's elemental composition by relating characteristic line intensities of the material's constituents. LIBS measurements have been performed on various materials[1–6] including solid[7–9] and liquid steel.[10,11] Values for limits of detection (LOD) achieved with LIBS analysis of liquid steel under atmospheric conditions are, e.g., 3 μg/g for C and 8.5 μg/g for Ni.[12] The LIBS results can vary depending on the laser parameters and the ambient atmospheric conditions during the plasma expansion.[13–15]

In the present paper we report on rapid *in situ* analysis of liquid metal melts under reduced ambient pressure by LIBS using a system that was developed in the frame of a co-operation of VOEST-ALPINE Industrieanlagenbau and the Johannes-Kepler University in Linz. The experimental setup is designed for field applications and was tested at a metallurgic vacuum-degassing (VD) and a vacuum-induction-melting (VIM) device at the steel mill of Böhler Edelstahl in Kapfenberg.

EXPERIMENTAL SETUP

For the field experiments we used a transportable prototype system that was developed from the setup described in our former publication.[16] The beam of a Q-switched Nd:YAG laser (wavelength 1064 nm, pulse length 5 to 7 ns, pulse energy about 350 mJ) was guided via a mirror arm (similar to that described in Ref. 17) to a gas-flushed window of the vacuum device and focused onto the surface of the sample by a concave spherical mirror (diameter, 60 mm) in the arm with a focal length adapted to the distance of the mirror to the steel bath in the different experiments (about 4 and 2.5 m, respectively). The typical laser fluences ϕ at the surface were between 5 and 10 J/cm^2, corresponding to laser-light intensities of several 100 MW/cm^2. These intensities were high enough to induce plasma formation above the surface. The emitted light of the plasma was collected by the concave mirror in the articulated arm and guided back. Then it was focused onto the entrance slit of a 0.5 m Czerny–Turner optical grating spectrometer. The resulting spectra were recorded, integrated on the gated detector over 100 to 300 pulses, read out, and analyzed on a computer. As described in Ref. 16 in greater detail, the measurements were performed using a grating with 2400 lines/mm. With the lowest number of laser pulses (100 at a repetition rate of 20 Hz), the analysis of each element takes about 7 s.

Received 7 July 2003; accepted 2 December 2003.
* Author to whom correspondence should be sent.

0003-7028/04/5804-0457$2.00/0

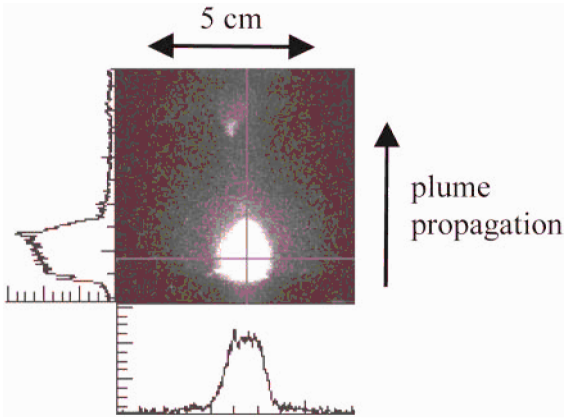

FIG. 1. Time-resolved photograph (gate 5 ns) of the plume with a delay $t = 1$ μs after the laser pulse (solid steel target, KrF excimer laser, background pressure $p(\mathrm{Ar}) = 1$ mbar, laser energy $E = 36$ mJ). The inserts show the intensity distribution along the cross-hairs indicated in the figure.

LASER-INDUCED BREAKDOWN SPECTROSCOPY UNDER REDUCED PRESSURE

The laser-induced vaporization of the material and the subsequent plasma formation and optical breakdown above the sample surface typically occur within some ten picoseconds.[18] The hot and radiative plasma then expands into the semi-space above the target, as is indicated in Fig. 1. Immediately after the laser pulse, the spectrum shows broad emission bands with a thermal background; later, the light emitted by the plasma consists mainly of sharp atomic or ionic emission lines, which decay with time. Therefore, all spectra were recorded for 5 μs starting with a delay of 1 μs after the laser pulse.

The plume propagation can be described over a wide range of parameters by a generalized shock wave expansion model.[18,19] In the course of expansion, the energy is redistributed between the thermal and kinetic energies of the plume and (internal and external) shock waves. The plume is decelerated and heated due to the counter-pressure of the ambient gas. At a certain distance from the target, the plume stops (and slightly contracts).

The absolute values of the stopping distance and the stopping time are proportional to $p^{-1/3}$. In laboratory tests, e.g., we measured for a solid steel target and a Nd:YAG laser pulse energy of 240 mJ at $p = 2$ mbar and a stopping time of about 80 μs (with a stopping distance of a few cm), while at $p = 20$ mbar and $p = 100$ mbar the stopping time was about 40 μs and 20 μs, respectively (with correspondingly smaller characteristic dimensions of the plasma plumes). As a consequence, the thermal energy density of the plume and therefore the absolute and relative intensity of various atomic or ionic transition lines depend on the ambient pressure. Similar to the results reported in Ref. 13, we found that at low pressures the detected intensities can be too small to perform a LIBS analysis for a given laser energy. The pressure used in metallurgic vacuum devices is in this critical low-pressure range. A final proof of principle for liquid steel analysis under reduced pressure had to be performed in a field experiment.

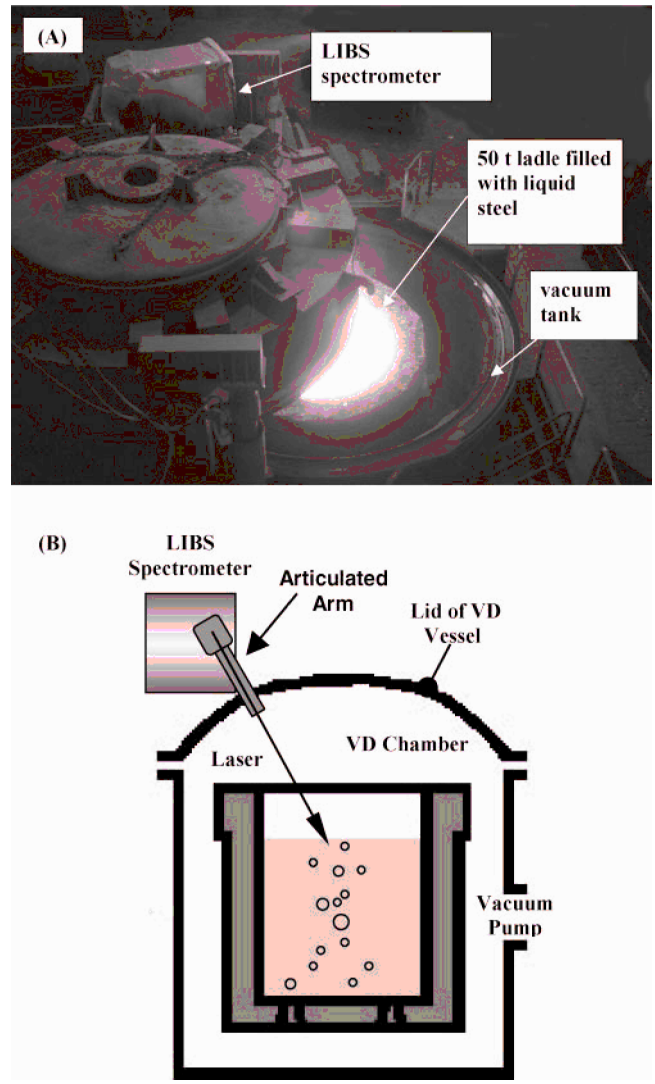

FIG. 2. LIBS spectrometer mounted on the lid of a VD vessel: (**A**) photograph with open lid, (**B**) schematic setup with closed lid.

EXPERIMENTS WITH A VACUUM-DEGASSING (VD) VESSEL

The transportable equipment was mounted on the hydraulic lid of a VD vessel in a special steel melt shop connected to the vacuum tank by a window (Fig. 2). The diameter of the vacuum tank was about 4 m. The distance between the focusing mirror and the surface of the liquid melt in the 50 t ladle was also on the order of 4 m and varied, depending on the actual filling of the ladle. For the treatment, the lid is moved hydraulically onto the vacuum tank and the vessel is pumped down to a pressure of about 1 mbar. From below the ladle can be flushed with either Ar or N_2, which is bubbling through the liquid melt resulting in an open, almost slag-free surface in the middle of the steel bath, onto which the laser was focused. However, the open surface is still very variable and splashy due to bubbles. Additionally, the fill level of the ladles differs considerably from heat to heat, which leads to a variation of the laser-spot size at the melt surface. The spot-size determines, together with other parameters such as laser-pulse energy and length or the melt temperature, what amount of material is ablated and how

much energy is coupled into the plasma. This, again, influences the result of the LIBS measurement.

All together, 25 heats were continuously analyzed during a program of two weeks. The heats were of different composition. By comparison with the chemical analysis provided by the laboratory located at the steel mill, calibration curves for several elements could be prepared. The chemical analysis used for comparison is based on samples taken by expendable samplers immediately after each VD treatment (at ambient pressure and without flushing). These samples are routinely analyzed for process- and quality-control purposes in the steel mill by standard techniques (e.g., spark-emission spectroscopy). Considering the harsh environmental conditions, the results of the evaluation of the LIBS spectra were, especially for the determination of the relative content of Cr, very satisfactory. Figure 3A shows the comparison of the LIBS results to the standard laboratory analysis for 12 different stainless steel heats in the VD-vessel. The Cr content of the heats varied from 0.51 to 15.71 wt % according to the standard laboratory analysis. The inset shows the spectral region used for Cr (of a heat with a Cr content of 1.7 wt %). As a measure for the relative content we took the intensity ratio of the indicated Cr and Fe lines, where the intensities were integrated over the line profiles. The error bars show the standard deviation of typically 5 analyses of one heat.

The LIBS analysis results for Mn in liquid steel (heats with a Mn content between 0.02 and 1.52 wt %) were subject to larger fluctuations from heat to heat in comparison with laboratory chemical analysis results. Spectral region and LIBS analysis emission lines are shown in the inset of Fig. 3B. The precision of the analysis of the single heats is quite good. However, the correlation to laboratory analysis, especially between 0.2 and 0.4 wt %, is poor. Here, the influence of interfering element lines and of parameters such as fill level and liquid-steel temperature may be more pronounced. In slag spectra we also found (relatively small) peaks at the position of the Fe 322.2 nm line and the Mn line at 323.1 nm, which had significantly different intensity ratios than the peaks in LIBS spectra from the melt. This was not the case for the Cr line at 434.5 nm and the Fe line at 440.5 nm, which were used to evaluate the Cr content. Hence, the poor correlation for Mn may indicate that there is always some slag present in the stirred liquid steel bath. This may be overcome by single-shot LIBS analysis (and not integrating the signal of 100 pulses) and by classifying each spectrum with respect to the detection of slag or steel. The classification could be done by identifying lines of components present in higher amounts only in slag (e.g., Ca). The slag spectra would then be excluded from the analysis.

For the LIBS analysis of Ni in a VD vessel (heats with a Ni content between 0.08 and 3.56 wt %) using the described setup, large deviations appear in the higher concentration range of around 3 wt %. Nevertheless, in the low concentration range, the reproducibility and accuracy are good. Again, the considered emission lines are indicated in the inset of Fig. 3C.

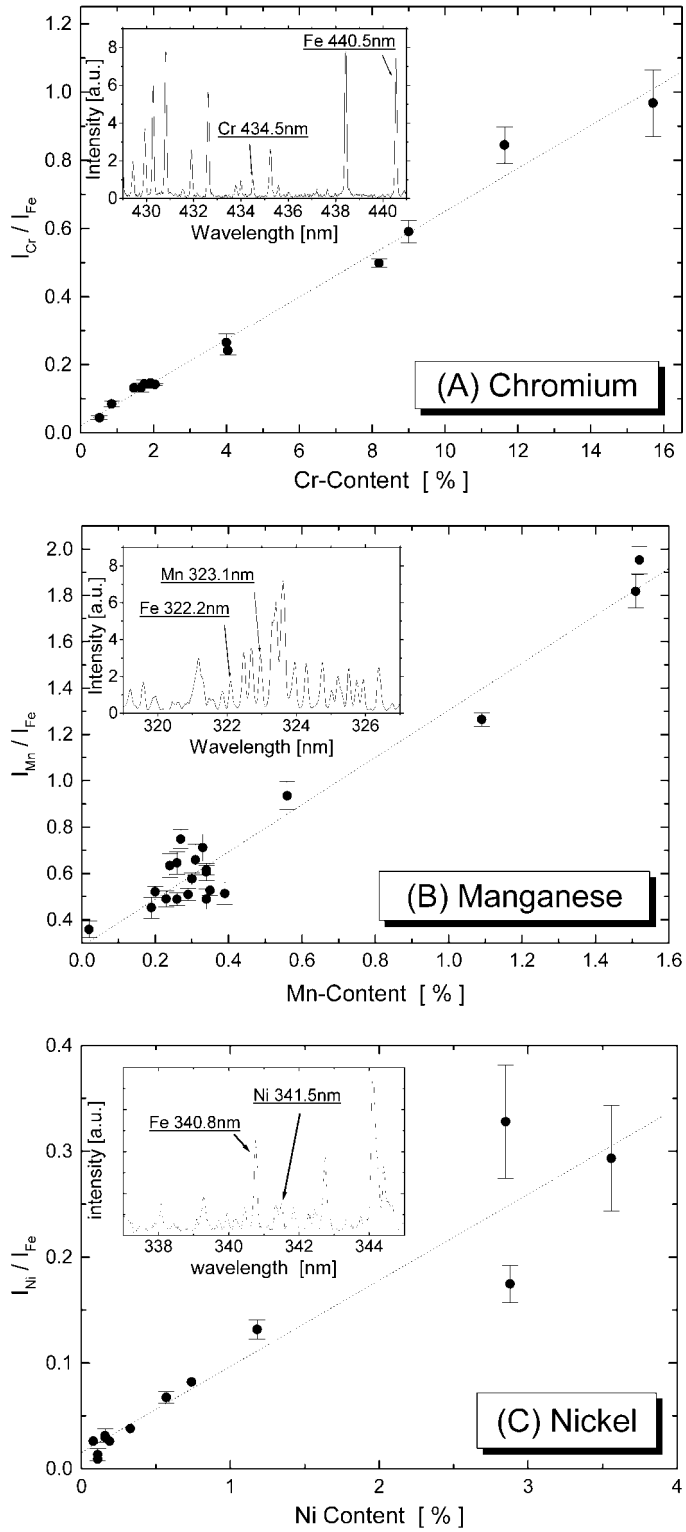

FIG. 3. Comparison of *in situ* LIBS results in a VD vessel with standard laboratory analysis: (**A**) Cr, (**B**) Mn, and (**C**) Ni (Insets: evaluated spectral lines).

IN SITU ANALYSIS OF LIQUID METAL IN A VACUUM-INDUCTION-MELTING (VIM) FURNACE

In a second on-site measurement series, the prototype was tested at a VIM furnace. Similar to the VD-treatment, a ladle containing the melt is evacuated to degas the liq-

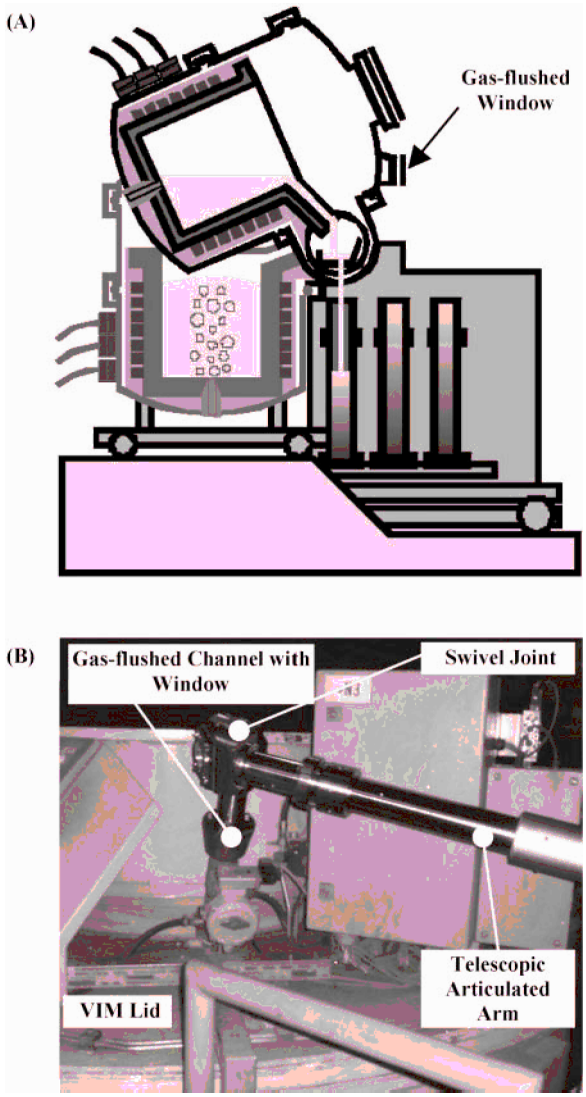

FIG. 4. (**A**) Schematic of a VIM furnace: treatment and casting. (**B**) Photograph of the articulated arm mounted to the gas-flushed window at a VIM furnace.

uid steel or several other types of alloys (e.g., a nickel-based alloy). Additionally, this metallurgical device is equipped with a combined inductive heating and stirring facility to heat and melt solid starting substances and for homogenizing the melt. The schematic of the VIM furnace is depicted in Fig. 4A. To cast the content of the ladle into ingots, the whole chamber can be tilted. One can also see the coils of the inductive heater and stirrer wrapped around the crucible. Solid steel ingots and scrap are inductively molten in the VIM furnace and alloyed to meet the demanded narrow margins of the final chemical composition. To maintain an inert atmosphere (usually Ar) at a pressure of around 0.2 mbar, the introduction of alloy substances is done through a vacuum-sluice. Sluices are also used for the measurement of the steel bath temperature and the drawing of samples for chemical analysis by special probes. When inductive stirring is active, a vortex is imposed on the melt and the thin slag layer on top of the metal bath is pushed to the rim of the ladle. Thus, in the center a slag-free liquid metal surface is again present. As in the VD measurements, a

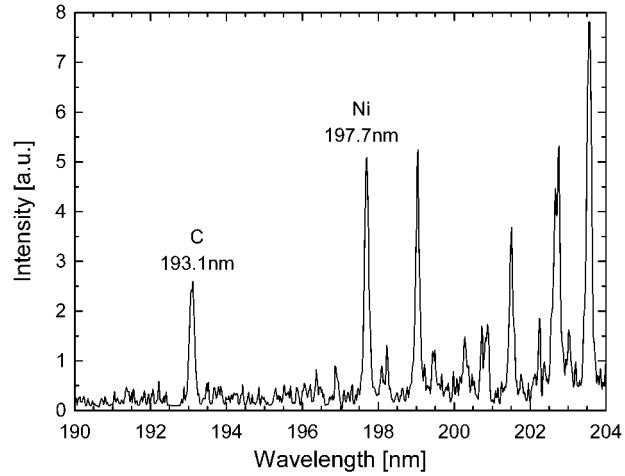

FIG. 5. Spectrum of LIBS measurements of a liquid Ni alloy in a VIM furnace.

gas-flushed channel mounted on the lid provides the optical access to the melt surface via a window, as shown in Fig. 4A. The LIBS prototype is optically linked to this channel by an articulated arm, which consists of two swivel joints connected by a set of telescopic tubes (see Fig. 4B). The diameter of the crucible in the vacuum tank was about 1.2 m with a depth of 1.5 m, and the distance of the melt surface to the window was about 2.5 m.

A Ni based alloy containing 74 wt % Ni, 0.063 wt % C, and around 20 wt % Cr was analyzed over a time period of 30 min during vacuum treatment and stirring in an Ar pressure of 0.22 mbar. In the same spectral region of the carbon emission line (C(I) at 193.1 nm) a Ni line (Ni(I) at 197.7 nm) could be identified (Fig. 5). The intensities (integrated over the line profiles) of these lines are plotted versus time in Fig. 6. Conditions were stable throughout the whole measurement time (i.e., constant pressure and bath temperature). The precision of these measurements seems to be rather low. A tendency towards lower carbon line intensity is recognizable, whereas the LIBS signal of Ni seems to stay constant over a long period of time. However, there are some oscillations in the line intensity with a period of several measurement

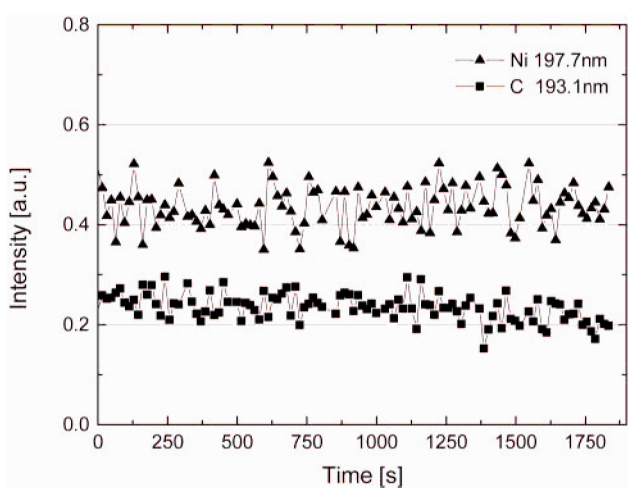

FIG. 6. Intensities of C and Ni lines in LIBS measurements of a liquid Ni alloy in a VIM furnace.

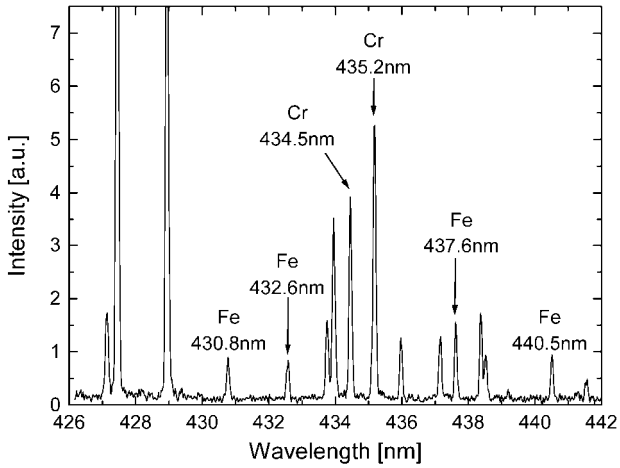

FIG. 7. LIBS spectrum of liquid steel in a VIM furnace.

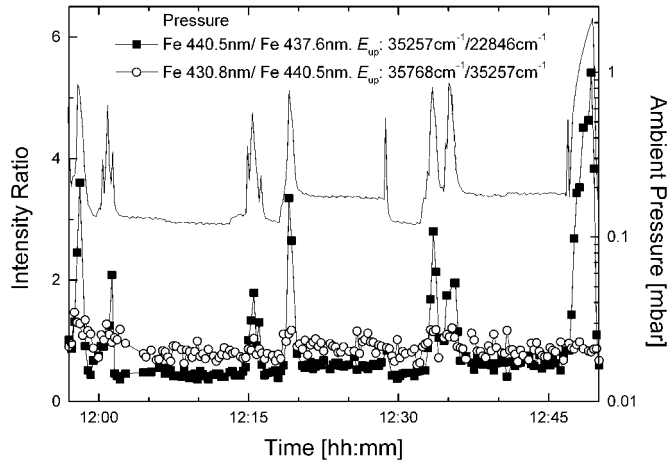

FIG. 8. Effect of the ambient pressure on the relative intensities of three Fe lines from Fig. 7.

cycles. This cannot be explained by an arbitrary signal fluctuation. Possibly, the origin of these oscillations is concentration gradients in the liquid metal bath, which are known from the literature.[20] The vortex structure induced by the inductive stirring and its speed of rotation could then be responsible for the oscillations in the C and Ni LIBS signal.

In the course of the vacuum treatment, the pressure undergoes certain fluctuations, especially when a vacuum-sluice must be opened for, e.g., temperature measurement. As expected from the previous considerations about the plume expansion, this variation in ambient pressure influenced the result of the LIBS analysis. A LIBS measurement (in the spectral region typically used for Cr analysis) on a steel alloy, containing 12.5 wt % Cr and 8.1 wt % Ni as well as other trace elements, is presented in Fig. 7. There is a strong dependence between the ambient Ar pressure and the intensity ratio of the lines shown in the graph. Considering the difference in upper energy E_{up} levels of the transition lines, the origin of the pressure dependence is very likely to be the changing plasma temperature, which is lower at lower pressures due to the larger spatial extension of the plume. The lower plasma temperature results in a decreased intensity of the lines with high E_{up} due to a reduced thermal population density according to the Boltzmann distribution. There is a very clear correlation between the relative intensities of spectral lines with different E_{up} and the ambient pressure, while lines with similar E_{up} show nearly no such dependences. This is demonstrated for the ratios of three Fe lines in Fig. 8. These effects have to be certainly compensated for proper LIBS analysis in this pressure range.

Assuming thermal equilibrium and neglecting self-absorption effects, the plasma temperature can be evaluated from the information contained in the spectrum. If the oscillator strength and upper energy levels are known and are sufficiently widespread, a Boltzmann plot can be prepared. The temperature can then be extracted from the plot by evaluating its slope. Two Fe lines, having a relatively large difference in upper energy levels (Fe(I) 437.6 nm, E_{up} = 22846 cm^{-1}; and Fe(I) 432.6 nm, E_{up} = 36079 cm^{-1}) were considered for the plasma temperature evaluation. The result is a plasma temperature of about 2400 K at a pressure of 0.1 mbar and of 3200 K at 1 mbar, respectively. It must be mentioned that considering only two lines of the same ionization stage can give only a very crude estimation of the plasma temperature. The calculated absolute value of the temperature is rather low compared to the temperature of plasmas created by pulsed laser ablation in atmospheric pressure, which is on the order of 10^4 K and more. However, such a low plasma temperature at this stage of plasma expansion is not surprising, since the ambient pressure is in the 0.1 mbar range. At these conditions, the plasma expands rapidly and cools quickly.

The number of heats analyzed during the VIM measurement series was limited. Thus, the number of data was insufficient for the preparation of calibration curves. Nevertheless, the change in concentration of certain elements after adding alloying substances could be monitored. As an example, the LIBS analysis before and after the addition of Ti to a Ni alloy (same as in Figs. 7 and 8) is presented. The intensity of the Ti(I) emission line at 427.5 nm and of the Cr(I) line at 434.5 nm are monitored by means of the LIBS prototype. In Fig. 9 the intensities of the Cr and Ti emission lines are plotted versus time. During a vacuum treatment (taking 2.5 h),

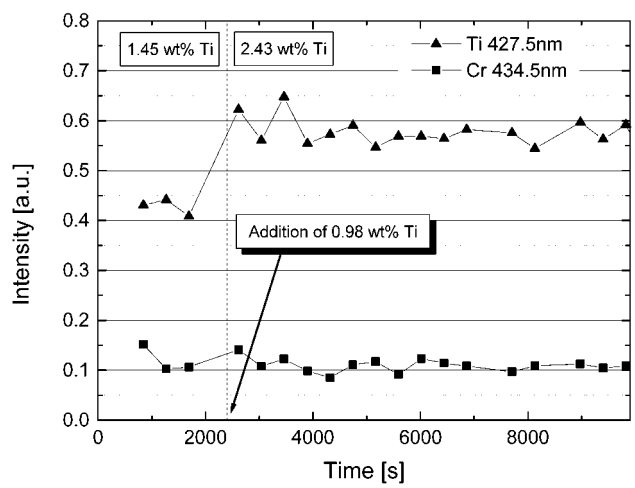

FIG. 9. Liquid steel analysis in a VIM furnace using LIBS: monitoring the addition of Ti.

the intensity of the Cr line turned out to be relatively stable after the addition of an alloying substance containing Ti. What can be seen clearly in the figure is the increase of the Ti line intensity after adding 0.98 wt % Ti to the liquid metal bath, which had an initial Ti content of 1.45 wt %. This shows that LIBS can also be used to monitor the chemical composition of metal alloys (a Ni alloy in this particular case) in VIM furnaces.

CONCLUSION

The measurements presented above have undoubtedly shown the applicability of LIBS in on-site liquid steel analysis in a metallurgical device under reduced pressure. Despite the harsh environment and the unfavorable conditions on the liquid steel surface, the prototype LIBS device has demonstrated the capability to perform an analysis of the melt composition. LIBS is a very promising and powerful tool for process control in an industrial environment. Focus must be laid on the reliability of the hardware and on improvements regarding LOD, accuracy, and precision in order to make LIBS a robust standard technique for material analysis. The concentration of Cr, Mn, and Ni in liquid steel could be determined with satisfactory precision. The influence of the ambient pressure on the expansion characteristics of the plasma plume and on the result of the LIBS analysis has been studied.

1. M. Sabsabi and P. Cielo, Appl. Spectrosc. **41,** 1042 (1987).
2. J. R. Wachter and D. A. Cremers, Appl. Spectrosc. **41,** 1042 (1987).
3. B. Bescos, J. Castona, and A. Gonzales Urena, Laser Chem. **16,** 75 (1995).
4. I. B. Gornushkin, J. E. Kim, B. W. Smith, S. A. Baker, and J. D. Winefordner, Appl. Spectrosc. **51,** 1055 (1997).
5. R. Sattmann, I. Mönch, H. Krause, R. Noll, S. Couris, A. Hatziapostolou, A. Mavromanolakis, C. Fotakis, E. Larrauri, and R. Miguel, Appl. Spectrosc. **52,** 456 (1998).
6. V. Tornari, V. Zafiropulos, A. Bonarou, N. A. Vainos, and C. Fotakis, Opt. Laser Eng. **34,** 309 (2000).
7. R. Sattmann, V. Sturm, and R. Noll, J. Phys. D: Appl. Phys. **28,** 2181 (1995).
8. C. Aragon, J. A. Aguilera, and F. Penalba, Appl. Spectrosc. **53,** 1259 (1999).
9. L. M. Cabalin, D. Romero, J. M. Baena, and J. J. Laserna, Surf. Interface Anal. **27,** 805 (1999).
10. C. Carlhoff, C. J. Lorenzen, K. P. Nick, and H. J. Siebenbeck, Proc. SPIE-Int. Soc. Opt. Eng. **1012,** 186 (1989).
11. R. Noll, R. Sattmann, V. Sturm, S. Lüngen, and H. von Wachtendonk, Stahl Eisen **107,** 57 (1997).
12. R. Noll, H. Bette, A. Brysch, M. Kraushaar, I. Mönch, L. Peter, and V. Sturm, Spectrochim. Acta, Part B **56,** 637 (2001).
13. V. Margetic, A. Pakulev, A. Stockhaus, M. Bolshov, K. Niemax, and R. Hergenröder, Spectrochim. Acta, Part B **55,** 1771 (2000).
14. J. A. Aguilera and C. Aragon, Appl. Phys. A **69,** S475 (1999).
15. S. Yalcin, D. R. Crosley, G. P. Smith, and G. W. Faris, Appl. Phys. B **68,** 121 (1999).
16. J. Gruber, J. Heitz, H. Strasser, D. Bäuerle, and N. Ramaseder, Spectrochim. Acta, Part B **56,** 685 (2000).
17. N. Ramaseder, J. Gruber, D. Bäuerle, and J. Heitz, international patent application WO0227301 (2002).
18. D. Bäuerle, *Laser Processing and Chemistry* (Springer, Heidelberg, 2000), 3rd ed.
19. N. Arnold, J. Gruber, and J. Heitz, Appl. Phys. A **69,** S87 (1999).
20. F. Oeters, *Metallurgie der Stahlherstellung (Metallurgy of Steel Production)* (Springer, Berlin, Heidelberg, 1989).